

# Progressive Subsampling for Oversampled Data - Application to Quantitative MRI

Stefano B. Blumberg<sup>1</sup>, Hongxiang Lin<sup>1,3</sup>, Francesco Grussu<sup>1,2</sup>,  
Yukun Zhou<sup>1</sup>, Matteo Figini<sup>1</sup>, and Daniel C. Alexander<sup>1</sup>

<sup>1</sup> University College London (UCL)

<sup>2</sup> Vall d'Hebron Barcelona Hospital

<sup>3</sup> Zhejiang Lab

hxlin@zhejianglab.edu.cn, stefano.blumberg.17@ucl.ac.uk

**Abstract.** We present PROSUB: PROgressive SUBsampling, a deep learning based, automated methodology that subsamples an oversampled data set (e.g. multi-channelled 3D images) with minimal loss of information. We build upon a recent dual-network approach that won the MICCAI Multi-Diffusion (MUDI) quantitative MRI measurement sampling-reconstruction challenge, but suffers from deep learning training instability, by subsampling with a hard decision boundary. PROSUB uses the paradigm of recursive feature elimination (RFE) and progressively subsamples measurements during deep learning training, improving optimization stability. PROSUB also integrates a neural architecture search (NAS) paradigm, allowing the network architecture hyperparameters to respond to the subsampling process. We show PROSUB outperforms the winner of the MUDI MICCAI challenge, producing large improvements  $>18\%$  MSE on the MUDI challenge sub-tasks and qualitative improvements on downstream processes useful for clinical applications. We also show the benefits of incorporating NAS and analyze the effect of PROSUB's components. As our method generalizes to other problems beyond MRI measurement selection-reconstruction, our code is [3].

**Keywords:** Magnetic Resonance Imaging (MRI) Measurement Selection, Recursive Feature Elimination, Neural Architecture Search

## 1 Introduction

Multi-modal medical imaging gives unprecedented insight into the microstructural composition of living tissues, and provides non-invasive biomarkers that hold promise in several clinical contexts. In particular, quantitative MRI fits a model in each pixel of a multi-channel acquisition consisting of multiple images each with unique contrast obtained by varying multiple MRI acquisition parameters, see e.g. [18]. This provides pixel-wise estimates of biophysical tissue properties [13]. In spite of this potential, comprehensively sampling high-dimensional acquisition spaces leads to prohibitively long acquisition times, which is a key barrier to more widespread adoption of qMRI in clinical use.

The MUlti-Diffusion (MUDI) MRI challenge [1,26] addressed this by providing data covering a densely-sampled MRI acquisition space i.e. 3D brain images with 1344 channels. The task was to reconstruct the full set of measurements from participant-chosen measurements as accurately as possible from a relatively small subsample. That involves two sub-tasks: selecting the most informative measurements, and reconstructing the full data set from them. The challenge winner was SARDU-Net [14,26,15], with a dual-network strategy, that respectively subsamples the measurements, then reconstructs the full dataset from the subsampled data. However, SARDU-Net selects different sets of measurements with a hard decision boundary on each training batch, altering the second network’s input across different batches. This can cause instability, seen in suppl. fig 3 and [21,8] show that similar approaches produce training instability. Furthermore, the popularity of paradigms such as recursive feature elimination (RFE), suggests that subsampling all of the measurements required immediately, is suboptimal. These two issues may lead to substandard performance.

Our implementation [3] is based on AutoKeras [20] and Keras-Tuner [25]. PROSUB outperforms the SARDU-Net and SARDU-Net with AutoKeras NAS by  $> 18\%$  MSE on the publicly available MUDI MRI challenge data [26,2]. We also show qualitative improvements on downstream processes: T2\* mapping and tractography, useful for clinical applications e.g. [23,17]. We also show that incorporating NAS improves task performance and examine the effect of PROSUB’s components. We release the code [3] as PROSUB is not limited for subsampling MRI data sets for microstructure imaging.

## 2 Related Work and Preliminaries

**Problem Setting** Suppose we have an oversampled dataset  $\mathbf{x} = \{\mathbf{x}_1, \dots, \mathbf{x}_n\} \in \mathbb{R}^{n \times N}$  where each sample has  $N$  measurements  $\mathbf{x}_i \in \mathbb{R}^N$ . The aim is to subsample  $M < N$  measurements  $\tilde{\mathbf{x}} = \{\tilde{\mathbf{x}}_1, \dots, \tilde{\mathbf{x}}_n\} \in \mathbb{R}^{n \times M}$ ,  $\tilde{\mathbf{x}}_i \in \mathbb{R}^M$ , with the same  $M$  elements of each  $\mathbf{x}_i$  in each  $\tilde{\mathbf{x}}_i$ . We aim to lose as little information as possible when choosing  $\tilde{\mathbf{x}}$ , thereby enabling the best recovery of the full data set  $\mathbf{x}$ . We therefore have two interconnected problems i) choosing which measurements to subsample, ii) reconstructing the original measurements from the subsampled measurements. We determine this by (i) by constructing a binary mask  $m$  containing  $M$  ones and  $N - M$  zeros so  $\tilde{\mathbf{x}} = m \cdot \mathbf{x}$ , (ii) with a neural network  $\mathcal{R}$ .

**SARDU-Net and Dual-Network Approaches** The SARDU-Net [14,26,15], which is used for model-free quantitative MRI protocol design and won the MUDI challenge [26], has two stacked neural networks, trained in unison. The first network learns weight  $w$  from  $\mathbf{x}$ .  $N - M$  smallest values of  $w$  are clamped to 0 and the first network subsamples and selects the measurements, by outputting  $\mathbf{x} \cdot w$ . The second network then predicts the original data from  $\mathbf{x} \cdot w$ . Related dual-network approaches include [10], which processed large point clouds, differing from our problem, as we do not assume our data has a spatial structure. We build upon the SARDU-Net and it is a baseline in our experiments.

**Recursive Feature Elimination (RFE)** One of the most common paradigms for feature selection is RFE, which has a long history in machine learning [29,5]. Recursively over steps  $t = 1, \dots, T$  RFE prunes the least important features based on some task-specific importance score, successively analyzing less and less features over successive steps. We use a form of RFE in PROSUB.

**Neural Architecture Search (NAS)** Selecting neural network architecture hyperparameters e.g. number of layers and hidden units, is a task-dependent problem, where the most common strategies are random search [7] or grid search [22]. NAS approaches, see e.g. [11], outperform classical approaches with respect to time required to obtain high-performing models. PROSUB uses a generic NAS paradigm which optimizes network architectures over successive steps  $t = 1, \dots, T$  in an outer loop. In an inner loop, with fixed architecture (and fixed  $t$ ), we perform standard deep learning training across epochs  $e = 1, \dots, E$ , caching network training and validation performance  $r_t^e$  after each epoch. At the end of step  $t$ , the previous losses  $\{r_j^i : i \leq E, j \leq t\}$  are used to update the network architectures for step  $t + 1$ . Our implementation is based on AutoKeras [20] NAS, with Keras-Tuner [25], which has good documentation and functionality.

### 3 Methods

We address the interdependency of the sampling-reconstruction problem with a dual-network strategy in section 3.1, illustrated in fig 1. In section 3.2 we progressively construct our mask  $m$ , used to subsample the measurements. PROSUB has an outer loop: steps  $t = 1, \dots, T$  where we simultaneously perform NAS and RFE, choosing the measurements to remove via a score, averaged across the steps, whilst simultaneously updating the network architecture hyperparameters. For fixed  $t$ , we perform deep learning training as an inner loop across epochs  $e = 1, \dots, E$ , where we learn the aforementioned score and also progressively subsample the measurements. We summarize PROSUB in algorithm 1.

#### 3.1 Scoring-Reconstruction Networks

Inspired by [10,14], we use two neural networks, trained in unison, to address the interdependency of our two interconnected problems.

**Scoring Network** The first network  $\mathcal{S}_t$  learns a preliminary score with a sigmoid activation in its last layer, to weight each measurement:

$$s_t = \mathcal{S}_t(\mathbf{x}) \quad s_t \in (0, 2)^{n \times N}. \quad (1)$$

**Mask** As described in section 2, we use an array  $m_t \in [0, 1]^N$  as a mask

$$\tilde{\mathbf{x}}_t = m_t \cdot \mathbf{x} \quad (2)$$

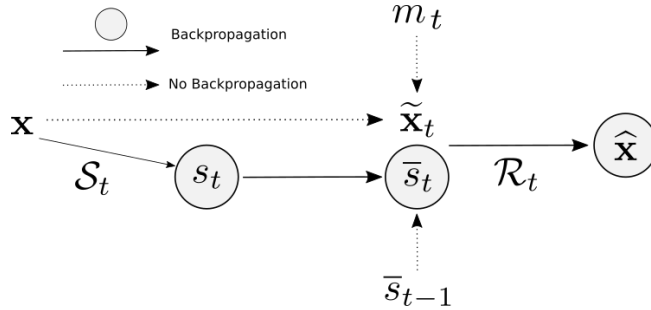


**Fig. 1.** The computational graph of PROSUB, for fixed step  $t = 1, \dots, T$  of neural architecture search (NAS) and recursive feature elimination (RFE). The subsampled data  $\tilde{\mathbf{x}}_t$  is a product of the input data  $\mathbf{x}$  and mask  $m_t$ . The Scoring Network  $S_t$  learns a preliminary score  $s_t$  for each measurement/channel of the input data  $\mathbf{x}$ . The final score for each measurement  $\bar{s}_t$  is a linear combination of  $s_t$  and an averaged score across previous steps ( $< t$ ):  $\bar{s}_{t-1}$ . The Reconstruction Network  $\mathcal{R}_t$  estimates the original data  $\hat{\mathbf{x}}$  from subsampled and normalized  $\tilde{\mathbf{x}}_t \cdot \bar{s}_t$ .

to subsample the measurements. We describe in section 3.2, how we progressively and manually set  $m_t$  to have  $N - M$  entries with 0.

**Average Measurement Score** To score each measurement in step  $t$ , we use an exponential moving average, commonly used in time-series analysis (e.g [16]), across the scores of previous steps  $\bar{s}_1, \dots, \bar{s}_{t-1}$  and  $s_t$ , to obtain a better estimate of the score and reduce the effect of the current learnt score  $\sigma_t$ , if network performance is poor. With moving average coefficient hyperparameter  $\alpha_t$  we calculate

$$\bar{s}_t = \alpha_t \cdot s_t + (1 - \alpha_t) \cdot \bar{s}_{t-1} \quad (3)$$

and we use  $\alpha_t = \frac{T-t}{T-1}$ . The averaged score  $\bar{s}_t$  is used to weight the subsampled measurements and to construct the mask (described in section 3.2).

**Reconstruction Network** The second network  $\mathcal{R}_t$  takes the weighted subsampled measurements to estimate  $\mathbf{x}$  with  $\hat{\mathbf{x}}$ , then passed through *Loss* (we use  $L^2$ )

$$L = \text{Loss}(\hat{\mathbf{x}}, \mathbf{x}), \quad \hat{\mathbf{x}} = \mathcal{R}_t(\tilde{\mathbf{x}}_t \cdot \bar{s}_t) \quad (4)$$

and the gradients from  $L$  are then backpropagated through  $\mathcal{R}_t, S_t$ .

### 3.2 Constructing the Mask to subsample the Measurements

We construct a mask  $m_t^e$ , used to subsample the measurements in section 2 and eq. 2. We progressively set  $N - M$  entries of  $m_t^e$  to zero, across NAS and RFE outer loop steps  $t = 1, \dots, T$  and deep learning training inner loop  $e = 1, \dots, E$ . We refer algorithm 1 for clarity.

---

**Algorithm 1** PROSUB: PROgressive SUBsampling for Oversampled Data
 

---

**Data and Task:**  $\mathbf{x} = \{\mathbf{x}_1, \dots, \mathbf{x}_n\}$ ,  $\mathbf{x}_i \in \mathbb{R}^N$ ,  $M < N$   
**Training and NAS:**  $1 \leq E_d \leq E$ ,  $1 < T_1 < T$ ,  $NAS \leftarrow AutoKeras$   
**Scoring and RFE:**  $\alpha_t \leftarrow \frac{T-t}{T-1}$ ,  $D_t \leftarrow \approx \frac{N-M}{T-T_1+1}$   
**Initialize:**  $m_1 \leftarrow [1]^N$ ,  $\tilde{m}, \bar{s}_0 \leftarrow [0]^N$

- 1: **for**  $t \leftarrow 1, \dots, T_1, \dots, T$  **do** ▷ RFE and NAS steps
- 2:   **if**  $1 \leq t < T_1$  **then**
- 3:      $D = \emptyset$  ▷ No measurements to subsample
- 4:   **else if**  $T_1 \leq t \leq T$  **then** ▷ Subsampling stage
- 5:      $D = \underset{j=1, \dots, D_t}{\operatorname{argsmin}} \{\bar{s}_t[j] : m_t[j] = 1\}$  ▷ Measurements to subsample Eq. 5
- 6:   **end if**
- 7:   **for**  $e \leftarrow 1, \dots, E_d, \dots, E$  **do** ▷ Training and validation epoch
- 8:      $m_t^e \leftarrow \max\{m_t - \frac{(e-E_d)\mathbb{1}_{e-E_d}}{E_d} \cdot \mathbb{1}_{i \in D}(i), 0\}$  ▷ Compute mask Eq. 6
- 9:      $s_t^e = \mathcal{S}(\mathbf{x})$ ,  $\tilde{\mathbf{x}}_t = m_t^e \cdot \mathbf{x}_t$  ▷ Forward pass Eq. 1,2
- 10:      $\bar{s}_t = \alpha_t \cdot s_t + (1 - \alpha_t) \cdot \bar{s}_{t-1}$  ▷ Average measurement score Eq. 3
- 11:      $r_t^e \leftarrow L(\tilde{\mathbf{x}}, \mathbf{x})$ ,  $L = L(\tilde{\mathbf{x}}, \mathbf{x})$ ,  $\hat{\mathbf{x}} = \mathcal{R}_t(\tilde{\mathbf{x}} \cdot \bar{s}_t)$  ▷ Forward/backward pass Eq.4
- 12:   **end for**
- 13:   Use NAS,  $\{r_j^i : i \leq E, j \leq t\}$ , to calculate  $\mathcal{R}_{t+1}, \mathcal{S}_{t+1}$  ▷ Update architectures
- 14:    $m_{t+1} \leftarrow m_t^E$ , *cache*  $\bar{s}_t$
- 15: **end for**
- 16: **return**  $m_T, \bar{s}_T, \mathcal{R}_T$  – use as described in section 2

---

**Outer Loop: Choosing the Measurements to Remove** Following standard practise in RFE e.g. [29,5], we remove the measurements recursively, in our case, across steps  $t = 1, \dots, T$  in alg.-line 1. We split the RFE in two stages, by choosing a dividing step, hyperparameter  $1 < T_1 < T$ .

In the first stage  $t = 1, \dots, T_1$  the optimization procedure learns scores  $\bar{s}_t$  and optimizes the network architectures via NAS. In alg.-line 3, we choose no measurements to subsample ( $D = \emptyset$ ) thus the mask  $m_t^e = m_t$  is fixed in alg.-line 8.

In the second stage  $t = T_1, \dots, T$ , we perform standard RFE. We first choose a hyperparameter  $D_t \in \mathbb{N}$  – the number of measurements to subsample in step  $t$ . In this paper, we remove the same number of measurements per step, so  $D_t \approx \frac{M-N}{T-T_1+1}$ . In alg.-line 5 we then choose the measurements to remove in RFE step  $t$ , which correspond to those with the lowest scores

$$D = \underset{j=1, \dots, D_t}{\operatorname{argsmin}} \{\bar{s}_t[j] : m_t[j] = 1\}, \quad m_t \in \{0, 1\}^N \quad (5)$$

where here  $m_t$  indicates whether the measurement has been removed in previous steps  $< t$ . Our rationale is since the subsampled measurements are weighted by the score, as inputs to the reconstruction network in eq. 4, setting lowest-scored values to 0 may have small effect on the performance:  $L$  in eq. 4.

**Inner Loop: Progressively Subsampling the Measurements by Altering the Mask During Training** Given  $D$  – computed in the outer loop in alg.-line 5 we progressively manually alter the mask  $m_t^e$  in the inner loop of deep

learning training alg.-line 7. This progressively sets the value of these measurements to 0 in  $\tilde{\mathbf{x}}_t$ . We are inspired by [21,8] which used a similar approach to improve training stability. We choose the number of epochs across which we alter the mask as a hyperparameter:  $E_d < \frac{E}{2}$ . We then alter the mask across  $e = E_d, \dots, 2 \cdot E_d - 1 \leq E$ :

$$m_t^e = \max \left\{ m_t - \frac{(e - E_d) \mathbb{I}_{e-E_d}}{E_d} \cdot \mathbb{I}_{i \in D}(i), 0 \right\} \quad (6)$$

which is used in eq. 2 and alg.-line 8.

## 4 Experiments and Results

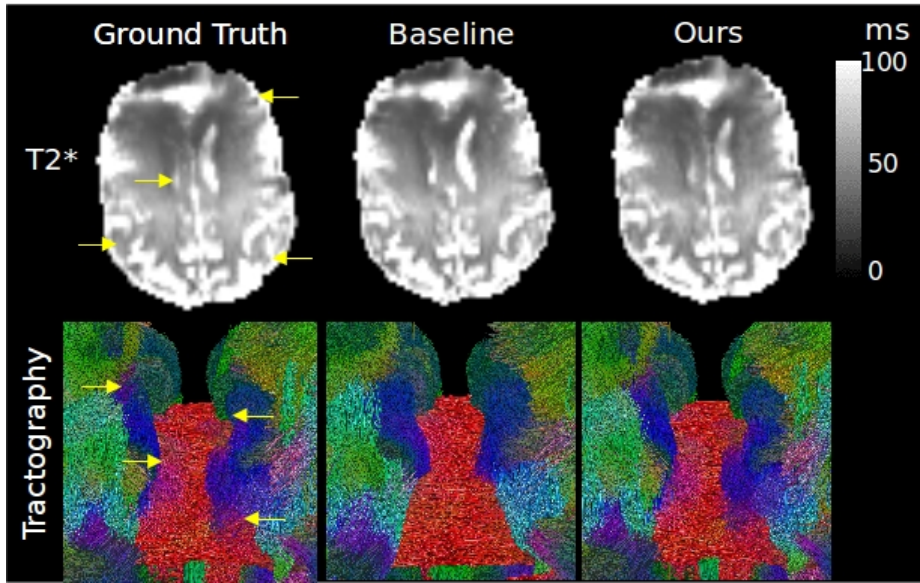
**Table 1.** Whole brain Mean-Squared-Error between  $N = 1344$  reconstructed measurements and  $N$  ground-truth measurements, on leave-one-out cross validation on five MUlti-Diffusion (MUDI) challenge subjects. The SARDU-Net won the MUDI challenge.

		MUDI Challenge M for $N = 1344$			
		500	250	100	50
SARDU-Net-v1 [14,26]	Baseline	$1.45 \pm 0.14$	$1.72 \pm 0.15$	$4.73 \pm 0.57$	$5.15 \pm 0.63$
SARDU-Net-v2 [4,15]	Baseline	$0.88 \pm 0.10$	$0.89 \pm 0.01$	$1.36 \pm 0.14$	$1.66 \pm 0.10$
SARDU-Net-v2-BOF [4,15]	Baseline	$0.83 \pm 0.10$	$0.86 \pm 0.10$	$1.30 \pm 0.12$	$1.67 \pm 0.12$
SARDU-Net-v2-NAS	Baseline	$0.82 \pm 0.13$	$0.99 \pm 0.12$	$1.34 \pm 0.26$	$1.76 \pm 0.24$
PROSUB w/o NAS	Ours	$0.66 \pm 0.08$	$0.67 \pm 0.09$	<b><math>0.88 \pm 0.07</math></b>	$1.54 \pm 0.11$
PROSUB	Ours	<b><math>0.49 \pm 0.07</math></b>	<b><math>0.61 \pm 0.11</math></b>	$0.89 \pm 0.11$	<b><math>1.35 \pm 0.11</math></b>

		No. samples M for $N = 1344$			
		40	30	20	10
SARDU-Net-v1 [14,26]	Baseline	$6.10 \pm 0.79$	$21.0 \pm 6.07$	$19.8 \pm 9.26$	$22.8 \pm 6.57$
SARDU-Net-v2 [4,15]	Baseline	$1.95 \pm 0.12$	$2.27 \pm 0.20$	$3.01 \pm 0.45$	$4.41 \pm 1.39$
SARDU-Net-v2-BOF [4,15]	Baseline	$1.86 \pm 0.18$	$2.15 \pm 0.23$	$2.61 \pm 0.24$	$3.74 \pm 0.66$
SARDU-Net-v2-NAS	Baseline	$2.23 \pm 0.22$	$6.00 \pm 7.14$	$2.82 \pm 0.41$	$4.27 \pm 1.66$
PROSUB w/o NAS	Ours	$1.81 \pm 0.18$	$2.18 \pm 0.17$	$2.72 \pm 0.34$	$3.91 \pm 0.22$
PROSUB	Ours	<b><math>1.53 \pm 0.05</math></b>	<b><math>1.87 \pm 0.19</math></b>	<b><math>2.50 \pm 0.40</math></b>	<b><math>3.48 \pm 0.55</math></b>

**MUDI Dataset and Task** Data of images from 5 subjects are from the MUDI challenge [1,26], publicly available [2]. Data features a variety of diffusion and relaxometry (i.e. T1 and T2\*) contrasts, and were acquired with the ZEBRA MRI technique [18]. The total acquisition time for these oversampled data sets was  $\approx 1h$ , corresponding to the acquisition of  $N = 1344$  measurements in this (dense) parameter space, resulting in 5, 3D brain images with 1344 channels (here unique diffusion- T2\* and T1- weighting contrasts), with  $n \approx 558K$  brain voxels. Detailed information is in [18,26]. We used the same task as the MICCAI MUDI challenge [26], where the participants were asked to find the most informative subsets of size  $M = 500, 250, 100, 50$  out of  $N$ , while also estimating the fully-sampled signals from each of these subsets, and the evaluation is MRI signal prediction MSE.



**Fig. 2.** Qualitative comparison of downstream processes of the reconstructed  $N = 1344$  measurements on a random test subject. T2\* and tractography have useful clinical applications e.g. [23,17]. Additional images and further details in suppl. fig 4.

The winner of the original challenge [1,26] was the aforementioned SARDU-Net [14,26]. In this paper, we also consider smaller subsets  $M = 40, 30, 20, 10$ .

**Experimental Settings** We did five-fold cross validation using two separate subjects for validation and testing. We compare PROSUB and PROSUB w/o NAS with four baselines: i) SARDU-Net-v1: winner of the MUDI challenge [14,26]; ii) SARDU-Net-v2: latest official implementation of (i) [4,15]; iii) SARDU-Net-v2-BOF: five runs of (ii) with different initializations, choosing the best model from the validation set; iv) SARDU-Net-v2-NAS: integrating (ii) with AutoKeras NAS. We also examined the effect of PROSUB’s components in suppl. table 2. To reduce total computational time with NAS techniques, we performed all of the tasks in succession. We first use algorithm 1 with  $T_1, T, M = 4, 8, 500$ , then take the final model, as initialization for algorithm 1 with  $T_1, T, M = 1, 5, 250$ , performing this recursively for  $M = 100, 50, 40, 30, 20, 10$ , using the best model for each different  $M$ . Consequently, SARDU-Net-v2-BOF and the NAS techniques in table 1 are trained for approximately the same number of epochs. We performed a brief search for NAS hyperparameters. All hyperparameters are in suppl. table 3.

**Main Results** We present quantitative results in table 1 and note PROMUSUB’s large improvements  $>18\%$  MSE over all four baselines on the MUDI challenge sub-tasks. Using the Wilcoxon one-sided signed-rank test, a non-parametric statistical test comparing paired brain samples, our methods improvements have

p-values of  $7.14\text{E}-08$ ,  $9.29\text{E}-07$ ,  $3.20\text{E}-06$ ,  $9.29\text{E}-07$  over the four respective baselines with Bonferroni correction, thus are statistically significant. We provide qualitative comparisons on a random test subject in figures 2,4 on downstream processes that are useful in clinical applications e.g. [23,17].

## 5 Discussion

The SARDU-Net-v2-NAS, generally underperforms the SARDU-Net w/o NAS. By examining network performance during NAS (e.g. like suppl. fig 3), this is due to SARDU-Net performance being unstable due to its hard measurement selection and fragile to changes in architecture. Passing poor results to the NAS update then reduces the effectiveness of the NAS in identifying high-performing architectures for small  $M$ . In contrast, PROSUB’s progressive subsampling allows the NAS to identify better architectures than the SARDU-Net-v2-NAS. PROSUB is also able to outperform the PROSUB w/o NAS i.e. here, the NAS is able to identify better performing architectures. We analyze the effect of PROSUB’s components in the suppl. table 2.

In future work, we could add an additional cost function to address the cost of obtaining specific combination of measurements from sets of MRI acquisition parameters; and develop a novel NAS algorithm to account for the concurrence of the subsampling process and architecture optimization. Our approach extends to many other quantitative MRI applications e.g. [6,9,13], other imaging problems e.g. [27] and wider feature selection/experiment design problems e.g. [24,28].

## Acknowledgements

We thank: Tristan Clark and the HPC team (James O’Connor, Edward Martin); MUDI Organizers (Marco Pizzolato, Jana Hutter, Fan Zhang); Amy Chapman, Luca Franceschi and Shinichi Tamura. Funding details SB: EPSRC and Microsoft scholarship, EPSRC grants M020533 R006032 R014019, NIHR UCLH Biomedical Research Centre, HL: Research Initiation Project of Zhejiang Lab (No.2021ND0PI02), FG: Fellowships Programme Beatriu de Pinós (2020 BP 00117), Secretary of Universities and Research (Government of Catalonia).

## References

1. MUlti-dimensional Diffusion (MUDI) MRI challenge 2019. <https://web.archive.org/web/20200209111131/http://cmic.cs.ucl.ac.uk/cdmri>
2. MUlti-dimensional Diffusion (MUDI) MRI challenge 2019 data. <https://www.developingbrain.co.uk/data/>
3. Our code. <https://github.com/sbb-gh/PROSUB>
4. SARDU-net official code. <https://github.com/fragrussu/sardunet>
5. Scikit-learn recursive feature elimination. [https://scikit-learn.org/stable/modules/generated/sklearn.feature\\_selection.RFE.html](https://scikit-learn.org/stable/modules/generated/sklearn.feature_selection.RFE.html)



6. Alexander, D.C.: A general framework for experiment design in diffusion mri and its application in measuring direct tissue-microstructure features. *Magnetic Resonance in Medicine* **60**(2), 439–448 (2008)
7. Bergstra, J., Bengio, Y.: Random search for hyper-parameter optimization. *Journal of machine learning research* **13**(Feb), 281–305 (2012)
8. Blumberg, S.B., Palombo, M., Khoo, C.S., Tax, C.M.W., Tanno, R., Alexander, D.C.: Multi-stage prediction networks for data harmonization. In: *Medical Image Computing and Computer Assisted Intervention (MICCAI)* (2019)
9. Brihuega-Moreno, O., Heese, F.P., Hall, L.D.: Optimization of diffusion measurements using cramer-rao lower bound theory and its application to articular cartilage. *Magnetic Resonance in Medicine* **50** (2003)
10. Dovrat, O., Lang, I., Avidan, S.: Learning to sample. In: *Proceedings of the IEEE Conference on Computer Vision and Pattern Recognition*. pp. 2760–2769 (2019)
11. Elsken, T., Metzen, J.H., Hutter, F.: Neural architecture search: A survey. *Journal of Machine Learning Research* **20**, 1–21 (2019)
12. Garyfallidis, E., et al.: Dipy, a library for the analysis of diffusion MRI data. *Frontiers in neuroinformatics* **8** (02 2014)
13. Grussu, F., Battiston, M., Veraart, J., Schneider, T., Cohen-Adad, J., Shepherd, T.M., Alexander, D.C., Fieremans, E., Novikov, D.S., Wheeler-Kingshott, C.A.G.: Multi-parametric quantitative in vivo spinal cord mri with unified signal readout and image denoising. *NeuroImage* **217**, 116884 (2020)
14. Grussu, F., Blumberg, S.B., Battiston, M., İanuş, A., Singh, S., Gong, F., Whitaker, H., Atkinson, D., Wheeler-Kingshott, C.A.M.G., Punwani, S., Panagiotaki, E., Mertzaniidou, T., Alexander, D.C.: SARDU-net: a new method for model-free, data-driven experiment design in quantitative mri. In: *International Society for Magnetic Resonance in Medicine (ISMRM)*, Abstract 1035 (2020)
15. Grussu, F., Blumberg, S.B., Battiston, M., Kakkar, L.S., Lin, H., İanuş, A., Schneider, T., Singh, S., Bourne, R., Punwani, S., Atkinson, D., Gandini Wheeler-Kingshott, C.A.M., Panagiotaki, E., Mertzaniidou, T., Alexander, D.C.: Feasibility of data-driven, model-free quantitative mri protocol design: Application to brain and prostate diffusion-relaxation imaging. *Frontiers in Physics* **9**, 615 (2021)
16. Hamilton, J.D.: *Time Series Analysis*. Princeton University Press, first edn. (1994)
17. Henderson, F., Abdullah, K.G., Verma, R., Brem, S.: Tractography and the connectome in neurosurgical treatment of gliomas: the premise, the progress, and the potential. *Neurosurgical focus* **48**(2) (2020)
18. Hutter, J., Slator, P.J., Christiaens, D., Teixeira, R.P.A., Roberts, T., Jackson, L., Price, A.N., Malik, S., Hajnal, J.V.: Integrated and efficient diffusion-relaxometry using zebra. *Scientific reports* **8**(1), 1–13 (2018)
19. Jeurissen, B., Tournier, J.D., Dhollander, T., Connelly, A., Sijbers, J.: Multi-tissue constrained spherical deconvolution for improved analysis of multi-shell diffusion mri data. *NeuroImage* **103**, 411–426 (2014)
20. Jin, H., Song, Q., Hu, X.: Auto-keras: An efficient neural architecture search system. In: *Proceedings of the 25th ACM SIGKDD International Conference on Knowledge Discovery & Data Mining*. pp. 1946–1956 (2019)
21. Karras, T., Aila, T., Laine, S., Lehtinen, J.: Progressive growing of gans for improved quality, stability, and variation. In: *International Conference on Learning Representations (ICLR)* (2018)
22. Larochelle, H., Erhan, D., Courville, A., Bergstra, J., Bengio, Y.: An empirical evaluation of deep architectures on problems with many factors of variation. In: *Proceedings of the 24th international conference on Machine learning*. pp. 473–480 (2007)

23. Lehericy, S., C, E.R., Goizet, Mochel, F.: MRI of neurodegeneration with brain iron accumulation. *Curr Opin Neurol*. **33**(4), 462–473 (2020)
24. Marinescu, R.V., Oxtoby, N.P., Young, A.L., Bron, E.E., Toga, A.W., Weiner, M.W., Barkhof, F., Fox, N.C., Golland, P., Klein, S., Alexander, D.C.: Tadpole challenge: Accurate alzheimer’s disease prediction through crowdsourced forecasting of future data. In: Rekik, I., Adeli, E., Park, S.H. (eds.) *Predictive Intelligence in Medicine*. pp. 1–10. Springer International Publishing, Cham (2019)
25. O’Malley, T., Bursztein, E., Long, J., Chollet, F., Jin, H., Invernizzi, L., et al.: Kerastuner. <https://github.com/keras-team/keras-tuner> (2019)
26. Pizzolato, M., Palombo, M., Bonet-Carne, E., Grussu, F., Ianus, A., Bogusz, F., Pieciak, T., Ning, L., Blumberg, S.B., Mertzanidou, T., Alexander, D.C., Afzali, M., Aja-Fernández, S., Jones, D.K., Westin, C.F., Rathi, Y., Baete, S.H., Cordero-Grande, L., Ladner, T., Slator, P.J., Christiaens, D., Thiran, J.P., Price, A.N., Seppehrband, F., Zhang, F., Hutter, J.: Acquiring and predicting MUlti-dimensional DIffusion (MUDI) data: an open challenge. In: *Computational Diffusion MRI (CDMRI)*
27. Prevost, R., Buckley, D.L., Alexander, D.C.: Optimization of the dce-ct protocol using active imaging. In: *2010 IEEE International Symposium on Biomedical Imaging (ISBI): From Nano to Macro* pp. 776–779 (2010)
28. van der Putten, P., van Somere, M.: CoIL challenge 2000: The insurance company case. Institute of Advanced Computer Science Technical Report (2000)
29. Zheng, A., Casari, A.: *Feature Engineering for Machine Learning: Principles and Techniques for Data Scientists*. O’Reilly (2018)

## Supplementary Materials

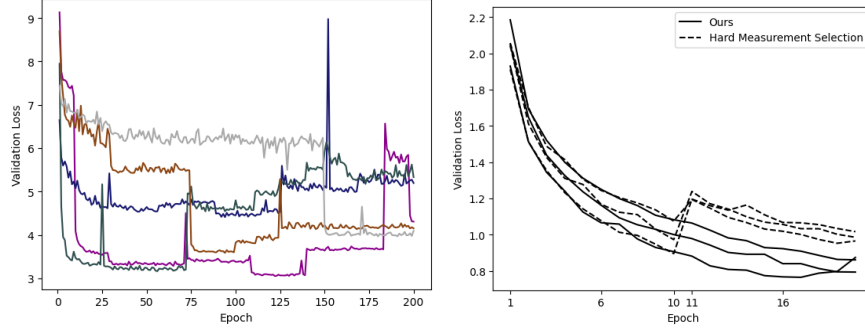


**Fig. 3.** Left: Training losses of the SARDUNet  $M = 10$  for different seeds/initializations (colors), the SARDU-Net selects different sets of measurements with a hard decision boundary on each training batch, altering the second network’s input across different batches, producing instability. Right: Progressively subsampling measurements during training eq. 6, compared to hard measurement selection (table 2 row 3).

**Table 2.** Ablation study of PROSUB’s components (top-to-bottom) i) not computing an average measurement score, ii) not using RFE, iii) not progressively subsampling measurements during training (also figure 3 right). No NAS, across five random seeds / initializations on a single validation subject,  $T_1, T, M = 2, 6, 50$ .

Formula Change	Val MSE
Alg.-line 10 is $\bar{s}_t = s_t, s_t \in \mathbb{R}^N$	$3.02 \pm 0.01$
$T_1 = T = 6, D[T_1] = M - N$	$1.86 \pm 0.03$
Alg.-line 8 is $m_t^e = \max \{m_t - (e - E_d)\mathbb{I}_{e-E_d} \cdot \mathbb{I}_{i \in D}(i), 0\}$	$1.52 \pm 0.03$
PROSUB w/o NAS	<b><math>1.47 \pm 0.08</math></b>

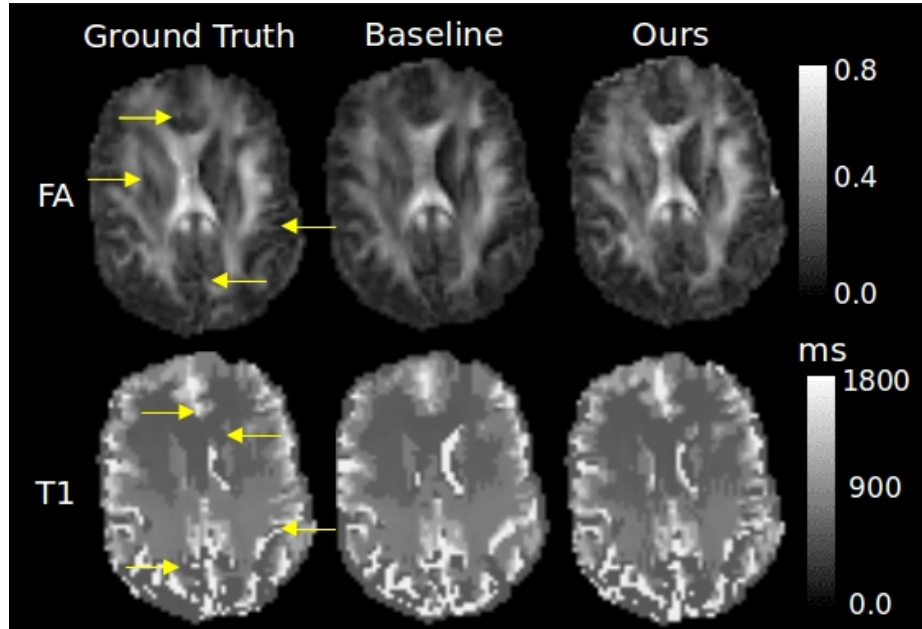


**Fig. 4.** Additional images and explanation of fig 2 . As the MUDI dataset provides combined diffusion and relaxometry information, to evaluate the practical impact of the different reconstructions we estimated T1 and T2\* values as well as DTI parameters with a dictionary-based fitting algorithm using DIPY [12]. To investigate the possibility to reconstruct fibre tracts from each set of data, we also performed whole-brain probabilistic tractography based on multi-shell multi-tissue constrained spherical deconvolution using the iFOD2 algorithm in mrtrix [19].

**Table 3.** All hyperparameters. We conducted a brief search for the NAS hyperparameters, which ex. dropout are the same between PROSUB and SARDUNet+NAS. SARDUNet w/o NAS baselines are from official implementation. 1st/2nd net. refers to respective fist/second network in the dual-network impelementations. ‘choices in’ means NAS can choose one of the following values e.g. #Layers in 1st net = 2 choices in {1, 2, 3} + 1 means the first layer in PROSUB  $S_t$  is replaced by 1, 2, 3 layers.

Hyperparameters	Value	SARDUNet	SARDUNet-NAS	PROSUB
$E$ , Optimizer, Learning Rate	200, ADAM, $1E-3$	✓	✓	✓
Batch Size, Weight Initialization	1500, He Normal	✓	✓	✓
Data Normalization	Max-99%	✓	✓	✓
	" measurement-wise			✓
$T_1, T$	4, 36 + 9		✓	✓
$\alpha_t, D_t, E_d$	$\frac{T-t}{T-1}, \frac{N-M}{T-T_1+1}, 20$			✓
NAS adapted from	AutoKeras w. Greedy (default) Strategy		✓	✓
#Layers in 1st/2nd net	3	✓		
	2 choices in {1, 2, 3} + 1		✓	✓
#Units in layer 1,2 1st net.	417, 333( $M = 500$ ) 1063, 781( $M < 500$ )	✓		
	2 choices in {128, 256, ..., 2048}		✓	✓
#Units in layer 1,2 2nd net.	781, 1063	✓		
	2 choices in {128, 256, ..., 2048}		✓	✓
	0.2	✓		
Dropout	4 choices in {0, 0.1, 0.2, 0.3, 0.4}		✓	
	0			✓